Electronic Supplementary Material (ESI) for ChemComm.
This journal is © The Royal Society of Chemistry 2018

Electronic Supplementary Information

Perovskite Oxide with Tunable Pore-Size Derived from a General Salt-Template Strategy as Highly Efficient Electrocatalyst for Oxygen Evolution Reaction

Haoran Yu,[a] Fuqiang Chu,[a] Xiao Zhou,[a] Junling Ji*, [a], Yang Liu,[a] Yunfei Bu,*, [b] Yong Kong,[a] Yongxin Tao,[a] Yongxin Li,[a] Yong Qin*, [a]

[a] Jiangsu Key Laboratory of Advanced Catalytic Materials and Technology, School of Petrochemical Engineering, Changzhou University, Changzhou 213164, China

[b] School of Environmental Science and Engineering, Nanjing University of Information Science & Technology, Nanjing, Jiangsu, 210044, China

*Corresponding authors:

E-mail: jijunling@cczu.edu.cn

E-mail: jpu441@yahoo.com

E-mail: qinyong@cczu.edu.cn

Experimental Section

Fabrication of Materials

The fabrication of porous perovskite oxide was performed by an inorganic salt-template strategy. Firstly, the $PrBa_{0.5}Sr_{0.5}Co_{1.5}Fe_{0.5}O_{5+\delta}$ (PBSCF) gel were prepared via a sol-gel method. Stoichiometric amounts of $Pr(NO_3)_3 \cdot 6H_2O$ (0.50 mmol), $Ba(NO_3)_2$ (0.25 mmol), $Sr(NO_3)_2$ (0.25 mmol), $Co(NO_3)_2 \cdot 6H_2O$ (0.75 mmol), and $Fe(NO_3)_3 \cdot 9H_2O$ (0.25 mmol) were dissolved in 3.6 mL deionized water to get a transparent solution, then, 2.4 mmol citric acid and 0.167 mL ethylene glycol were added into the solution. The mixture was heated at 70 ^oC for 2 hours to produce a viscous gel under magnetic stirring. Secondly, the gel was mixed with 20 g anhydrous K_3PO_4 powder which had been dried prior to use. The free water in the gel was absorbed by anhydrous K_3PO_4 to form hydrate K_3PO_4, while the gel was transformed into xerogel monolith. The xerogel monolith was first dried in oven, and then calcined at 600 ^oC for 4 hours following 900 ^oC for 4 hours in air. Finally, the calcined monolith was immersed in water to dissolve the K_3PO_4 template. The remained sendiment was centrifuged, and washed with water. After dried at 70 ^oC overnight, the final porous PBSCF was obtained and denoted as p-PBSCF. The fabrication of bulk PBSCF (b-PBSCF) was basically identical to that of p-PBSCF, except that the gel was dried and calcined directly, but need not use the anhydrous K_3PO_4 template. Similarly, the bulk and porous BSCF and LSC were prepared, labeled as b-BSCF, b-LSC, p-BSCF, and p-LSC.

Characterization

The powder X-ray diffraction (XRD, Rigaku D/max 2500PC diffractometer, Cu-Kα radiation) were used to confirm the crystalline phase of samples. The microstructure and morphology of p-PBSCF were observed by a field-emission scanning electron microscope (FESEM, Zeiss,

Germany) and transmission electron microscopy (TEM, JEOL JEM-2100F), and scanning transmission electron microscopy (STEM) fixed with a high-angle-annular-dark-field (HAADF) detector at 300 kV. Chemical analysis of the materials was accomplished by X-ray photoelectron spectroscopy (XPS, ESCALAB 250Xi, Thermo Fisher Scientific, USA). The Brunauer-Emmett-Teller (BET) surface area and pore distribution of the materials was measured using the N_2 adsorption/desorption analyzer (Micromeritics, USA). The electrochemical measurements including cyclic voltammetry and linear sweep voltammetry (LSV) were implemented on a CHI 660D electrochemical workstation interfaced with a rotating disk electrode (RDE, Pine Cooperation, USA).

Electrochemical measurements

The electrochemical measurements were conducted in an electrochemical cell equipped with the conventional three-electrode system. Typically, the rotating disk electrode (RDE) with the diameter of 3 mm (0.07 cm^2 in geometric area) was used as the working electrode. Pt plate electrode and the saturated calomel electrode (SCE) served as the counter electrode and the reference electrode, respectively. The catalyst ink was prepared by ultrasonically dispersing 4.0 mg catalyst, 1.0 mg conductive carbon black, and 20.0 μL Nafion solution (5 wt.%) in a mixed solvent containing 1.5 mL deionized water and 0.5 mL isopropanol. Then, 7 μl of catalyst ink was dropped onto RDE, which was dried in air at room temperature for 4 h to construct the work electrode. The loading of catalyst on the RDE is calculated to be 0.2 mg cm^{-2}. The potential versus SCE was converted into the corresponding potential versus reversible hydrogen electrode (RHE) according the equation $E_{vs\ RHE} = E_{vs\ SCE} + E^{\theta}_{SCE} + 0.059\ pH$ [1]. All potentials were iR-corrected to compensate the effect of solution resistance [2]. 0.1 M KOH aqueous solution (pH=13) was used as the electrolyte. To ensure the equilibrium potential of O_2/H_2O at 1.23 V

versus RHE, the electrolyte was saturated with O_2 for 20 minutes prior to use [3]. LSV measurements were performed with RDE at the rotation speed of 1600 rpm and scan rate of 10 mV s^{-1} from 1.2 V to 1.8 V versus RHE. The current-time tests were carried out at the current density of 10 mA cm^{-2}.

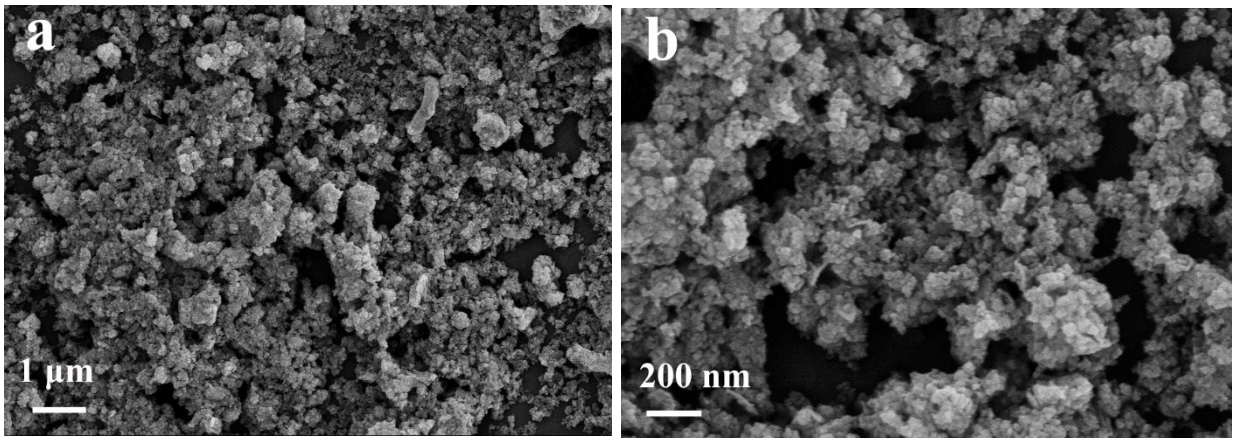

Fig. S1 SEM images of p-PBSCF

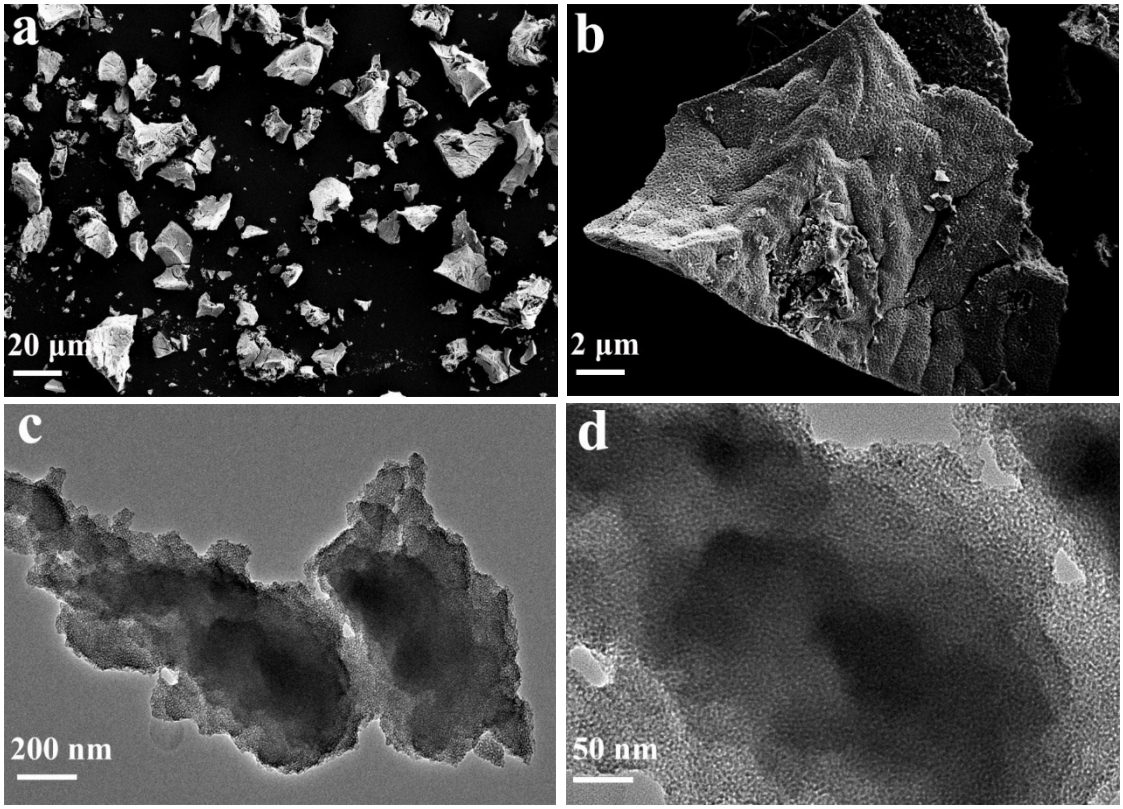

Fig.S2 SEM (a, b) and TEM (c, d) images of b-PBSCF.

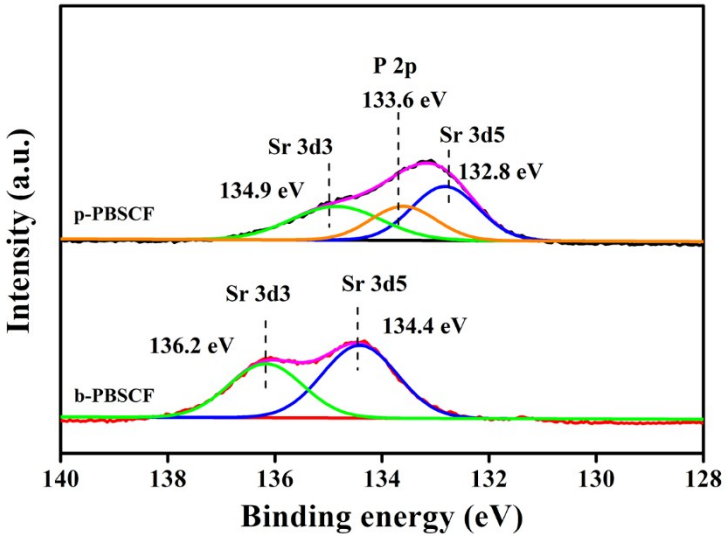

Fig.S3 The P 2p and Sr 3d XPS of the p-PBSCF and b-PBSCF.

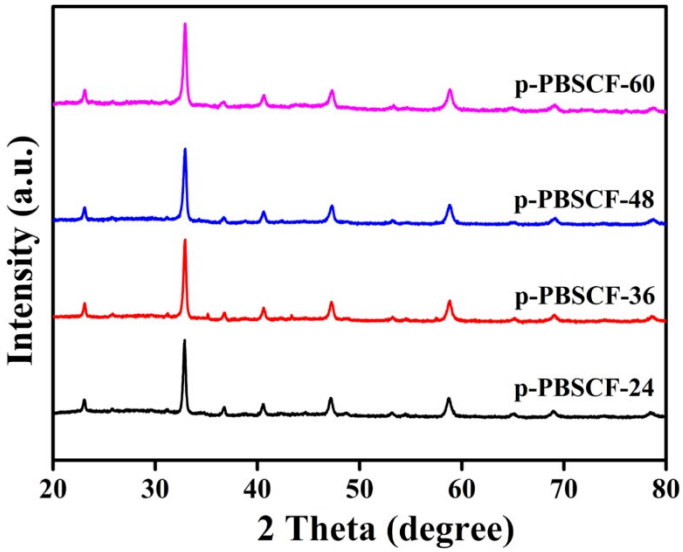

Fig. S4 The XRD patterns of p-PBSCF fabricated by various amount of K_3PO_4 template.

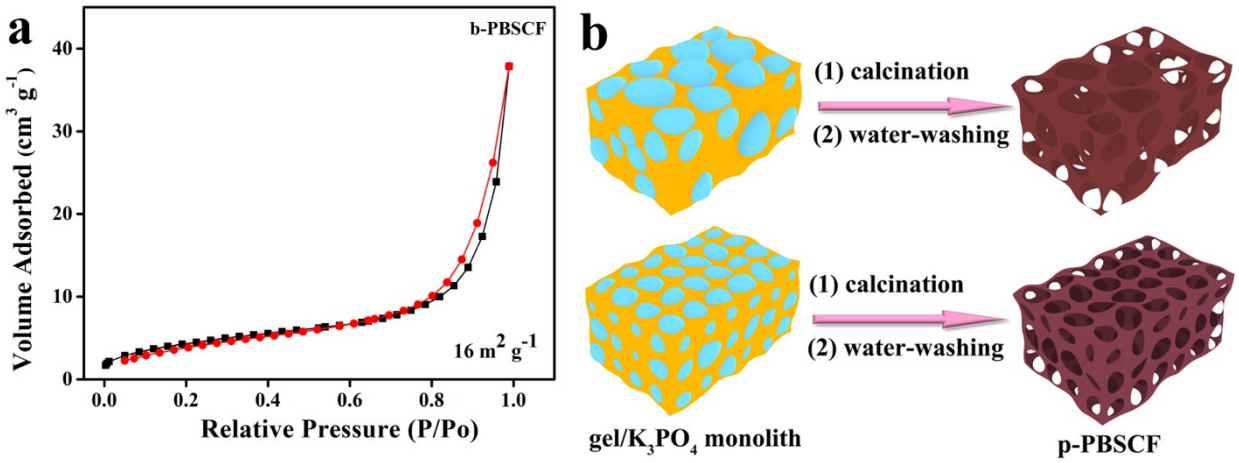

Fig.S5 (a) N_2 adsorption-desorption isotherms of the b-PBSCF, (b) mechanism of the pore size tuned by K_3PO_4 template, the high (up) and low (down) amount of K_3PO_4 added.

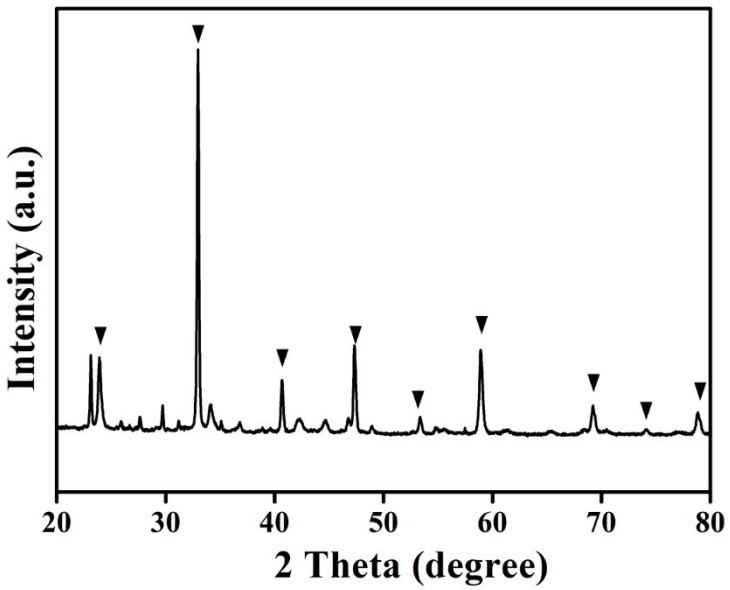

Fig. S6 XRD of p-PBSCF fabricated by $BaCl_2$ template.

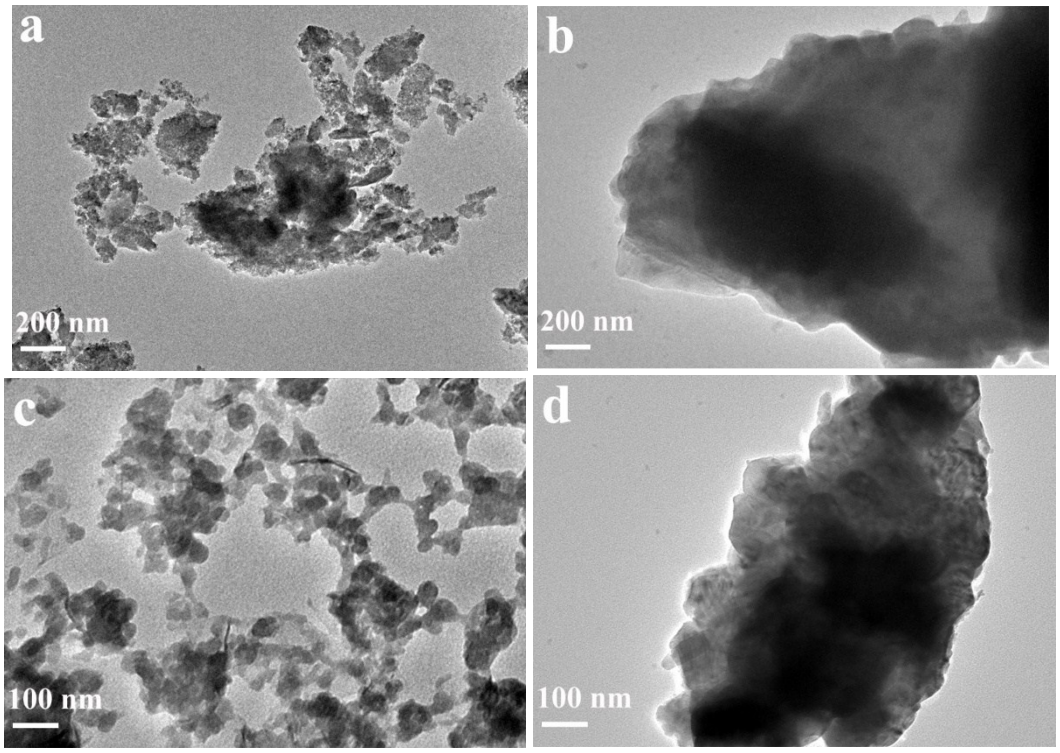

Fig. S7 TEM images of p-LSC (a), b-LSC (b), p-BSCF (c), and b-BSCF (d).

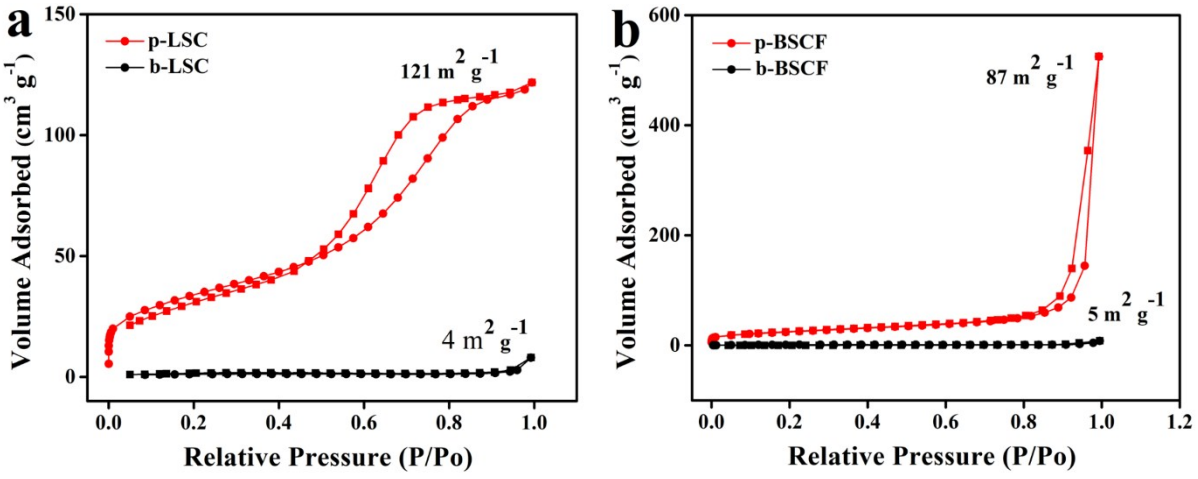

Fig. S8 N_2 adsorption-desorption isotherm of p-LSC, b-LSC, p-BSCF, and b-BSCF.

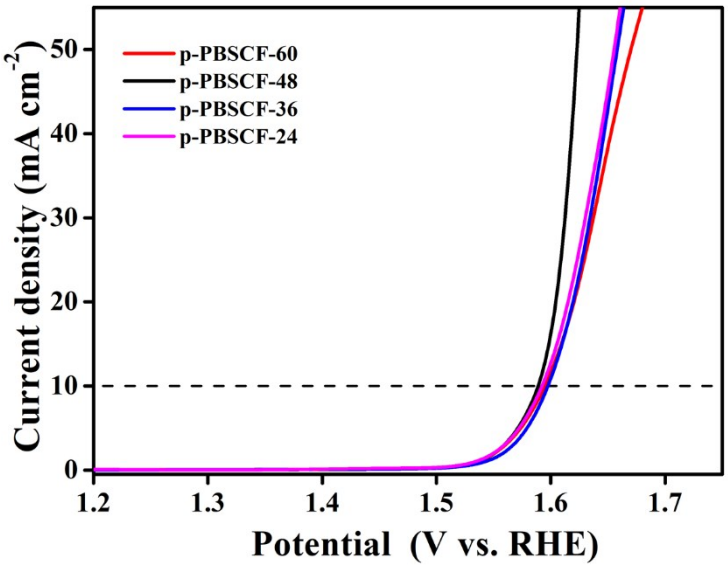

Fig. S9 OER activity of the p-PBSCF fabricated with various amount of K_3PO_4 template.

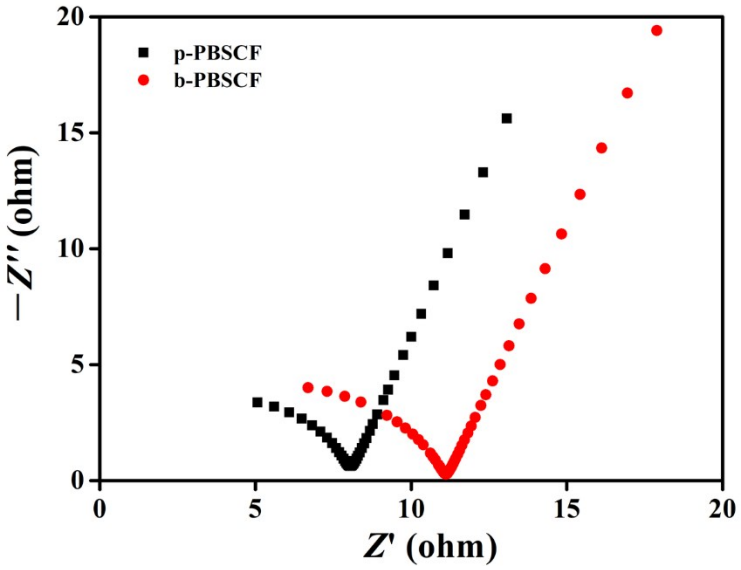

Fig. S10 EIS of p-PBSCF and the b-PBSCF.

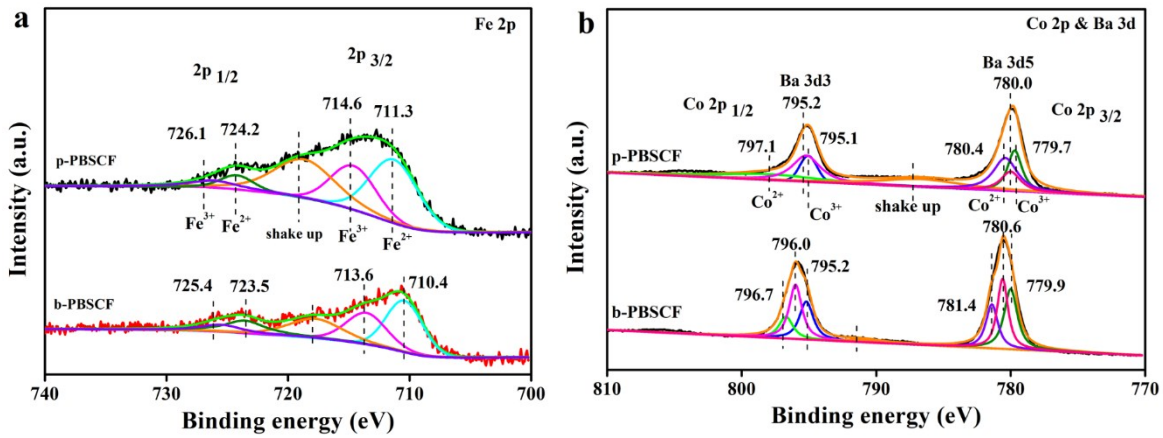

Fig. S11 The fine XPS of Fe 2p and Co 2p of P-PBSCF and b-PBSCF. After P-doping, Fe and Co shift to the higher valence state significantly.

Tab. S1 The comparison of the BET surface area of our fabricated p-PBSCF with those reported in literature.

Sample	Method	Template	BET ($m^2 g^{-1}$)	Ref.
p-PBSCF	Hard template	K_3PO_4	148	This work
$La_{0.6}Sr_{0.4}MnO_3$	Hard template	PMMA	42.1	[4]
$LaFeCoO_3$	Hard template	Porous carbon	49.3	[5]
$LaMnO_3$	Hard template	KIT-6	45	[6]
$LaMnO_3$	Hard and soft template	Lysine-aided	37.8	[7]
3DOM-m $La_{0.7}Ce_{0.3}CoO_3$	Hard and soft template	PMMA and P123	35.4	[8]
$La_{0.6}Sr_{0.4}Co_{0.2}Fe_{0.8}O_3$	Soft template	F-127	30	[9]
$LaMnO_3$	Soft template	CTBA	50	[9]
$La_{0.7}(Ba_{0.5}Sr_{0.5})_{0.3}Co_{0.8}Fe_{0.2}O_{3-\delta}$	Sol-gel		21.9	[10]
$La_{0.6}Sr_{0.4}MnO_3$	Sol-gel		42.1	[11]
$LaFeO_3$	Hydrothermal		25.8	[12]
$SrNb_{0.1}Co_{0.7}Fe_{0.2}O_{3-\delta}$	Electrospinning		45	[2]
$(La_{0.6}Sr_{0.4})_{0.95}Co_{0.2}Fe_{0.8}O_{3+\delta}$	Electrospinning		17.96	[13]
$PrBa_{0.5}Sr_{0.5}Co_{1.5}Fe_{0.5}O_{5+\delta}$	Electrospinning		18.81	[3]

Tab. S2 Comparison of OER performance in 0.1M KOH.

Catalyst	**Tafel slope** (**mV dec^{-1}**)	**η 10** (**mV**)	**Catalyst loading** (**mg cm^{-2}**)	**Ref.**
p-PBSCF	56	359	0.2	This work
P-doped $LaFeO_{3-\delta}$	50	460	0.255	[14]
$BaCo_{0.8}Zr_{0.1}Y_{0.1}O_3$	83	420	0.232	[15]
LP-$LaSr_3Co_{1.5}Fe_{1.5}O_{10-\delta}$	83.9	388	0.255	[16]
$La_{0.95}FeO_{3-\delta}$	48	410	0.232	[17]
$SrCo_{0.9}Ti_{0.1}O_{3-\delta}$	88	510	0.32	[18]
$Ba_{0.5}Sr_{0.5}Co_{0.8}Fe_{0.2}O_{3-\delta}$	94	500	0.232	[19]
$SrNb_{0.1}Co_{0.7}Fe_{0.2}O_{3-\delta}$	76	500	0.232	[19]
$LaCoO_3$	69	490	0.25	[20]

Reference

[1] S. Wang, L. Zhang, Y. Qin, D. Ding, Y. Bu, F. Chu, Y. Kong and M. Liu, *J. Power Sources*, 2017, **363**, 260.

[2] Y. Zhu, W. Zhou, Y. Zhong, Y. Bu, X. Chen, Q. Zhong, M. Liu and Z. Shao, *Adv. Energy Mater.*, 2017, **7**, 1602122.

[3] B. Zhao, L. Zhang, D. Zhen, S. Yoo, Y. Ding, D. Chen, Y. Chen, Q. Zhang, B. Doyle, X. Xiong and M. Liu, *Nat. Commun.*, 2017, **8**, 14586.

[4] H. Arandiyan, H. Dai, J. Deng, Y. Wang, S. Xie and J. Li, *Chem. Commun.*, 2013, **49**, 10748.

[5] H. Zhu, P. Zhang and S. Dai, *ACS Catal.*, 2015, **5**, 6370.

[6] Z. Sarshar, F. Kleitz and S. Kaliaguine, *Energy Environ. Sci.*, 2011, **4**, 4258.

[7] Y. Liu, H. Dai, Y. Du, J. Deng, L. Zhang and Z. Zhao, *Appl. Catal., B*, 2012, **119-120**, 20.

[8] H. Arandiyan, J. Scott, Y. Wang, H. Dai, H. Sun and R. Amal, *ACS Appl. Mater. Interfaces*, 2016, **8**, 2457.

[9] R. Chao, R. Munprom, R. Petrova, K. Gerdes, J. R. Kitchin, P. A. Salvador and J. Stevenson, *J. Am. Ceram. Soc.*, 2012, **95**, 2339.

[10] J. I. Jung, M. Risch, S. Park, M. G. Kim, G. Nam, H. Y. Jeong, Y. Shao-Horn and J. Cho, *Energy Environ. Sci.*, 2016, **9**, 176.

[11] H. Arandiyan, H. Dai, J. Deng, Y. Liu, B. Bai, Y. Wang, X. Li, S. Xie and J. Li, *J. Catal.*, 2013, **307**, 327.

[12] K. Ji, H. Dai, J. Deng, L. Song, S. Xie and W. Han, *J. Solid State Chem.*, 2013, **199**, 164.

[13] Y. Chen, Y. Bu, Y. Zhang, R. Yan, D. Ding, B. Zhao, S. Yoo, D. Dang, R. Hu, C. Yang and M. Liu, *Adv. Energy Mater.*, 2017, **7**, 1601890.

[14] Z. Li, L. Lv, J. Wang, X. Ao, Y. Ruan, D. Zha, G. Hong, Q. Wu, Y. Lan, C. Wang, J. Jiang and M. Liu, *Nano Energy*, 2018, **47**, 199-209.

[15] H. Liu, J. Yu, J. Sunarso, C. Zhou, B. Liu, Y. Shen, W. Zhou and Z. Shao, *Electrochim. Acta*, 2018, **282**, 324-330.

[16] S. Liu, H. Luo, Y. Li, Q. Liu and J.-L. Luo, *Nano Energy*, 2017, **40**, 115-121.

[17] Y. Zhu, W. Zhou, J. Yu, Y. Chen, M. Liu and Z. Shao, *Chem. Mater.*, 2016, **28**, 1691-1697.

[18] C. Su, W. Wang, Y. Chen, G. Yang, X. Xu, M. O. Tadé and Z. Shao, *ACS Appl. Mater. Interfaces*, 2015, **7**, 17663-17670.

[19] Y. Zhu, W. Zhou, Z.-G. Chen, Y. Chen, C. Su, M. O. Tadé and Z. Shao, *Angew. Chem. Int. Edit.*, 2015, **54**, 3897-3901.

[20] S. Zhou, X. Miao, X. Zhao, C. Ma, Y. Qiu, Z. Hu, J. Zhao, L. Shi and J. Zeng, *Nat. Commun.*, 2016, **7**, 11510.